

The statistical two-order and two-scale method for predicting the mechanics parameters of core-shell particle-filled polymer composites

Fei Han¹, Junzhi Cui² and Yan Yu¹

¹*Department of Applied Mathematics, Northwestern Polytechnical University, Xi'an, 710072 China*

²*Academy of Mathematics and System Sciences, Chinese Academy of Sciences, Beijing, 100080 China*

(Received December 13, 2007, Accepted May 12, 2008)

Abstract. The statistical two-order and two-scale method is developed for predicting the mechanics parameters, such as stiffness and strength of core-shell particle-filled polymer composites. The representation and simulation on meso-configuration of random particle-filled polymers are stated. And the major statistical two-order and two-scale analysis formulation is briefly given. The two-order and two-scale expressions for the strains and stresses of conventionally strength experimental components, including the tensional or compressive column, the twist bar and the bending beam, are developed by means of their classical solutions with orthogonal-anisotropic coefficients. Then a new effective mesh generation algorithm is presented. The mechanics parameters of core-shell particle-filled polymer composites, including the expected stiffness parameters, minimum stiffness parameters, and the expected elasticity limit strength and the minimum elasticity limit strength, are defined by means of the stiffness coefficients and elasticity strength criteria for core, shell and matrix. Finally, the numerical results for predicting both stiffness and elasticity limit strength parameters are compared with the experimental data.

Keywords: polymer matrix composites; finite element modeling (FEM); core-shell particle; elastic limit strength

1. Introduction

In recent years, the Core-shell Particle-filled Polymer Composites (CPPC for short) are extensively used in a variety of engineering and industrial products, such as adhesives, coatings, electronic products, electric apparatus, aircraft and aerospace, etc. A large number of studies on the properties of CPPC have been done. As we all known, the numerical modeling is important to predict the properties of materials. However, less numerical models for predicting the mechanics properties of CPPC were found due to its complex meso-configurations. In this paper, the Statistical Two-Order and Two-Scale Method (STOTSM for short) is presented in order to predict stiffness and strength parameters of CPPC.

The common character of CPPC is as follows: a large number of particles with various

morphologies in matrix materials subject to a certain random distribution model. Obviously, it is difficult to generate geometric and physical samples and finite element meshes not only by hands, but also by computers, owing to large computing capacity and complexity. Furthermore, the property prediction of CPPC, especially for mechanical strength and behavior, needs to generate a number of samples with randomly distributed particles by computer again and again. Consequently, it is important for predicting the property of CPPC to develop the fast and efficient methods for generating the samples with random distribution of complex particles, and then the FE meshes of the domain occupied by the sample.

Yu and Cui (2006) presented a new effective computer algorithm to produce the samples with the random distribution of a number of heterogeneous particles, which satisfies some specified probability model. There is also a FE partition method with tetrahedron elements for the geometric domain with randomly distributed particles was given in Li (2004). Both the methods were applied in calculating the constitutive parameters of shell-less particle-filled composites with statistical multi-scale methods. Li and Cui (2005) calculated stiffness parameters of composites with the particles obeyed to uniform random distribution using the statistical two-scale method. And Cui, Yu etc. Cui *et al.* (2007) improved the two-scale method to propose a two order and two-scale method for predicting the elastic limit strength parameters of the composites with the random distribution of a number of heterogeneous particles, and they also obtained the predicted results of valid elastic limit strength by practically computing. However, the predicting method for mechanics property of CPPC is rare. Therefore, in this paper a predicting method for the mechanics property with meso-configuration of CPPC was considered systematically on the basis of above works. Firstly, a new fast and effective algorithm is presented to construct geometric and physical model and generate meshes for CPPC. Secondly, STOTSM is adopted for calculating the stiffness and elastic strength parameters of CPPC. Finally, the predicted results are given.

The remainder of this paper is outlined as follows: In Section 2, the representing method and geometry modeling for meso-configuration of composites with random distribution of many particles are briefly illuminated, and then the statistical two-order and two-scale approximate formulas are expressed. And Section 3 is devoted to the expansions on the strain tensor for three kinds of conventional components made from CPPC. In Section 4 the mesh generation algorithm for the domain of CPPC and the computing procedure of STOTSM for both stiffness and strength parameters of CPPC are stated. And the numerical results for mechanics properties of different CPPC in three examples are displayed in Section 5. They show that the STOTSM is feasible and valid for the mechanics parameter prediction of the core-shell particle-filled polymer composites.

2. Statistical two-order and two-scale method

2.1 Representation for meso-configuration of polymers with random distribution of particles

For the composites with random distribution of a large number of particles, their configuration in meso-scale is described by some probability distribution model with ε -periodicity (Yu and Cui 2006). It supposes in paper Yu and Cui (2006) that in composites there exists a least constant ε such that the configuration of composites is regarded as the set of a great number of cells with ε -cube, shown in Fig. 1, the probability distributions of ellipsoids in any cells are the same. So the meso-configuration of the investigated composites is described by the probability distribution in a statistic

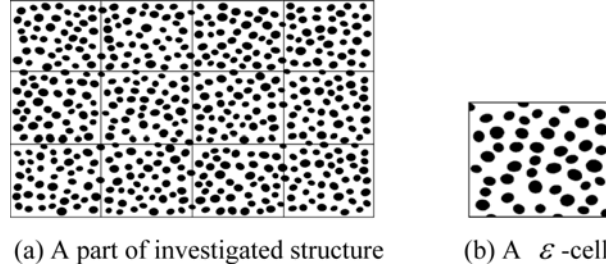


Fig. 1 The structure of composites with random distribution of particles

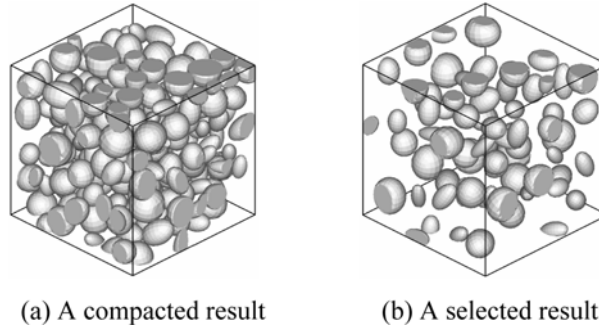


Fig. 2 The geometric sample with random distribution of ellipsoids

screen with ε -size, and then the ε -cells are arranged periodically to form a structure. However, the meso-configuration of CPPC is more complex. In the representation way (Yu and Cui 2006) every core-shell particle is represented by an ellipsoid and the normalized cell with lots of randomly distributed ellipsoids is constructed, shown in Fig. 2. Both the ‘compactness algorithm’ and ‘selection algorithm’ are given in Yu and Cui (2006).

In the compactness algorithm the randomly generated ellipsoids are arranged compactly over the entire cell, shown in Fig. 2(a). The selection algorithm is to choose such a part of ellipsoids that they obey a specified probability distribution, shown in Fig. 2(b). Then the shell for each core-shell particle is generated by extending or shrinking the long axis, middle axis and short axis of ellipsoid.

In a word, the above algorithms can generate the samples such that the following properties: The samples satisfy a specific random distribution model; They have the higher particle volume fraction; The shape parameters and orientation parameters of all ellipsoids also have complete randomness; The position parameters of all ellipsoids have better randomness.

2.2 Statistical two-order and two-scale approximate formulation for mechanics parameters

As the preceding representation shown, suppose that the structure Ω is made from the composite materials of random distribution model with small periodicity, and it is only composed of the entire ε -cells, shown in Fig. 1(a). Then $\Omega = \bigcup_{(\omega^s, t \in \mathbb{Z})} \varepsilon(Q^s + t)$, where εQ^s denotes an investigated screen

with ε -size, shown in Fig. 1(b); $\omega^s \in P$ is a sample obeying a given probability distribution model

P of particles in the whole structure; Z is the integer set; Q^s denotes a normalized cell; $\omega = \{\omega^s | x \in \varepsilon Q^s \subset \Omega\}$ in the entire structure.

From solid mechanics, for this kind of structure Ω , the elasticity problem can be expressed as the following virtual work equation

$$\int_{\Omega} \left(\frac{\partial v_i}{\partial x_j} + \frac{\partial v_j}{\partial x_i} \right) a_{ijhk}^{\varepsilon}(x, \omega) \left(\frac{\partial u_h^{\varepsilon}(x, \omega)}{\partial x_k} + \frac{\partial u_k^{\varepsilon}(x, \omega)}{\partial x_h} \right) d\xi = -4 \int_{\Omega} f_i(x) v_i dx \quad \forall v \in H_0^1(\Omega) \quad (1)$$

where $a_{ijhk}^{\varepsilon}(x, \omega)$ ($i, j, h, k = 1, 2, 3$) are the elastic coefficients with probability distribution P with small periodicity.

From (Li 2004), it was given that displacement vector is approximately expressed as follows

$$\mathbf{u}^{\varepsilon}(x, \omega) = \mathbf{u}^0(x) + \varepsilon \mathbf{N}_{\alpha_1}(\xi, \omega) \frac{\partial \mathbf{u}^0(x)}{\partial x_{\alpha_1}} + \varepsilon^2 \mathbf{N}_{\alpha_1 \alpha_2}(\xi, \omega) \frac{\partial^2 \mathbf{u}^0(x)}{\partial x_{\alpha_1} \partial x_{\alpha_2}} + \varepsilon^3 P_1(x, \xi, \omega) \quad (2)$$

where $\mathbf{u}^0(x)$ is the homogenization solution defined on global Ω and $\xi = \frac{x}{\varepsilon}$ denotes the local coordinates defined on 1-normalized cell Q , $\mathbf{N}_{\alpha_1}(\xi, \omega)$ and $\mathbf{N}_{\alpha_1 \alpha_2}(\xi, \omega)$ ($\alpha_1, \alpha_2 = 1, \dots, n$) are n -order matrix valued functions in unit cell Q . They have the below forms

$$\begin{aligned} \mathbf{N}_{\alpha_1}(\xi, \omega) &= \begin{pmatrix} \mathbf{N}_{\alpha_1 11}(\xi, \omega) & \cdots & \mathbf{N}_{\alpha_1 1n}(\xi, \omega) \\ \vdots & \cdots & \vdots \\ \mathbf{N}_{\alpha_1 n1}(\xi, \omega) & \cdots & \mathbf{N}_{\alpha_1 nn}(\xi, \omega) \end{pmatrix} \\ \mathbf{N}_{\alpha_1 \alpha_2}(\xi, \omega) &= \begin{pmatrix} \mathbf{N}_{\alpha_1 \alpha_2 11}(\xi, \omega) & \cdots & \mathbf{N}_{\alpha_1 \alpha_2 1n}(\xi, \omega) \\ \vdots & \cdots & \vdots \\ \mathbf{N}_{\alpha_1 \alpha_2 n1}(\xi, \omega) & \cdots & \mathbf{N}_{\alpha_1 \alpha_2 nn}(\xi, \omega) \end{pmatrix} \end{aligned} \quad (3)$$

and $\mathbf{N}_{\alpha_1}(\xi, \omega)$, $\mathbf{N}_{\alpha_1 \alpha_2}(\xi, \omega)$ and $\mathbf{u}^0(x)$ are determined as follows:

(1) For any sample $\omega^s \in P$, $\mathbf{N}_{\alpha_1 m}(\xi, \omega)$ ($\alpha_1, m = 1, \dots, n$) are the solutions of the following virtual work equation

$$\begin{aligned} \int_{Q^s} \left(\frac{\partial v_i}{\partial \xi_j} + \frac{\partial v_j}{\partial \xi_i} \right) a_{ijhk}(\xi, \omega^s) \left(\frac{\partial N_{\alpha_1 hm}(\xi, \omega^s)}{\partial \xi_k} + \frac{\partial N_{\alpha_1 km}(\xi, \omega^s)}{\partial \xi_h} \right) d\xi \\ = -4 \int_{Q^s} a_{ijm \alpha_1}(\xi, \omega^s) \frac{\partial v_i}{\partial \xi_j} dx \quad \forall v \in H_0^1(Q^s) \end{aligned} \quad (4)$$

(2) From $\mathbf{N}_{\alpha_1 m}(\xi, \omega)$, the homogenization elasticity tensor $\{\hat{a}_{ijhk}(\omega^s)\}$ depended on $\omega^s \in P$ is calculated

$$\hat{a}_{ijhk}(\omega^s) = \int_{Q^s} \left(a_{ijhk}(\xi, \omega^s) + a_{ijpq}(\xi, \omega^s) \frac{1}{2} \left(\frac{\partial N_{hpk}(\xi, \omega^s)}{\partial \xi_q} + \frac{\partial N_{hqk}(\xi, \omega^s)}{\partial \xi_p} \right) \right) d\xi \quad (5)$$

(3) According to Kolmogorov's strong law of large numbers the expected homogenization elasticity parameters $\{\widehat{a}_{ijhk}\}$ are evaluated by calculating $\hat{a}_{ijhk}(\omega^s)$ repeatedly

$$\widehat{a}_{ijhk} = \frac{\sum_{s=1}^M \hat{a}_{ijhk}(\omega^s)}{M}, \quad M \rightarrow +\infty \quad (6)$$

where M is the number of samples.

(4) For any sample $\omega^s \in P$, $\mathbf{N}_{\alpha_1 \alpha_2 m}(\xi, \omega^s)$, $(\alpha_1, \alpha_2, m = 1, \dots, n)$ are the solutions of the following virtual work equation

$$\begin{aligned} & \int_{Q^s} \left(\frac{\partial v_i}{\partial \xi_j} + \frac{\partial v_j}{\partial \xi_i} \right) a_{ijhk}(\xi, \omega^s) \left(\frac{\partial N_{\alpha_1 \alpha_2 hm}(\xi, \omega^s)}{\partial \xi_k} + \frac{\partial N_{\alpha_1 \alpha_2 km}(\xi, \omega^s)}{\partial \xi_k} \right) d\xi \\ &= -4 \int_{Q^s} \left[\left(\widehat{a}_{ijhk} - a_{i\alpha_2 m \alpha_1}(\xi, \omega^s) - a_{i\alpha_2 hk}(\xi, \omega^s) \frac{\partial N_{\alpha_1 hm}(\xi, \omega^s)}{\partial \xi_k} \right) v_i \right. \\ & \quad \left. + a_{ijh\alpha_2}(\xi, \omega^s) N_{\alpha_1 hm}(\xi, \omega^s) \frac{\partial v_j}{\partial \xi_i} \right] d\xi \quad \forall v \in H_0^1(Q^s) \end{aligned} \quad (7)$$

(5) $\mathbf{u}^0(x)$ is the solution of the homogenization problem defined on the global Ω with the expected homogenized elasticity parameters $\{\widehat{a}_{ijhk}\}$

$$\int_{\Omega} \left(\frac{\partial v_i}{\partial x_j} + \frac{\partial v_j}{\partial x_i} \right) \widehat{a}_{ijhk} \left(\frac{\partial u_h^0(x)}{\partial x_k} + \frac{\partial u_k^0(x)}{\partial x_h} \right) d\xi = -4 \int_{\Omega} f_i(x) v_i dx \quad \forall v \in H_0^1(\Omega) \quad (8)$$

(6) According to the elasticity theory, from above formula (2), the strains are evaluated approximately

$$\begin{aligned} \varepsilon(x, \omega) &= \frac{1}{2} \left(\frac{\partial u_h^0(x)}{\partial x_k} + \frac{\partial u_k^0(x)}{\partial x_h} \right) \\ &+ \sum_{l=1}^2 \varepsilon^l \sum_{\alpha_1 \dots \alpha_l = 1 \dots n} \frac{1}{2} \left[N_{\alpha_1 \dots \alpha_l hm}(\xi, \omega) \frac{\partial^{l+1} u^0(x)}{\partial x_{\alpha_1} \dots \partial x_{\alpha_l} \partial x_k} + N_{\alpha_1 \dots \alpha_l km}(\xi, \omega) \frac{\partial^{l+1} u^0(x)}{\partial x_{\alpha_1} \dots \partial x_{\alpha_l} \partial x_h} \right] \\ &+ \sum_{l=1}^2 \varepsilon^{l-1} \sum_{\alpha_1 \dots \alpha_{l-1} = 1 \dots n} \frac{1}{2} \left[\frac{\partial N_{\alpha_1 \dots \alpha_{l-1} hm}(\xi, \omega)}{\partial \xi_k} + \frac{\partial N_{\alpha_1 \dots \alpha_{l-1} km}(\xi, \omega)}{\partial \xi_h} \right] \frac{\partial^l u^0(x)}{\partial x_{\alpha_1} \dots \partial x_{\alpha_{l-1}}} \end{aligned} \quad (9)$$

(7) From Hooke's Law, the stresses are evaluated

$$\sigma_{ij}(x, \omega) = \widehat{a}_{ijhk} \varepsilon_{hk}(x, \omega) \quad (10)$$

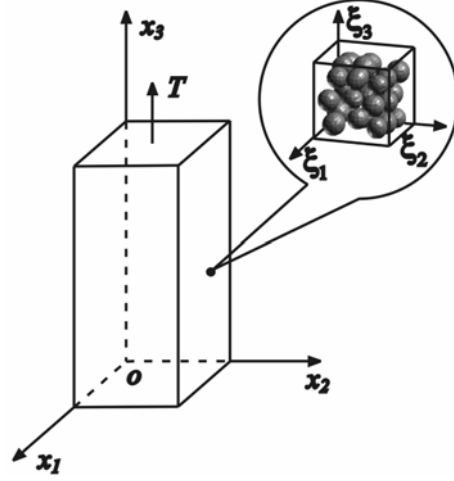


Fig. 3 Column with rectangular cross section

3. Calculation on mechanics parameters of CPPC

3.1 Formulation for the strains of some classic components

In this paper, three typical components are considered to evaluate the mechanical properties of CPPC, including the tensional or compressive column, the bending beam and the twist bar. From the two-order and two-scale asymptotic expression in section 2.2, the approximate analytic expression on the strains of these components is obtained.

a) Column tension

The tensile behavior of the column with rectangular cross section shown in Fig. 3, which is made from CPPC, is investigated. A denotes the area of cross section, L length of the column, $x_3 = 0$ fixed end and $x_3 = L$ loading end with loading T . From elasticity mechanics for the tension problem of the column with orthogonal-anisotropic material coefficients, its displacement solution is as follows

$$\left\{ \begin{array}{l} u_1^0 = -\frac{v_{13}}{E_{11}} p x_1 \\ u_2^0 = -\frac{v_{23}}{E_{22}} p x_2 \\ u_3^0 = \frac{p}{E_{33}} x_3 \end{array} \right. \quad (11)$$

where $p = T/A$, E_{11} , E_{22} , E_{33} , v_{13} and v_{23} are the homogeneous elasticity moduli of three axis directions and Poisson ratios, respectively.

Obviously, the above displacement solution $\mathbf{u}^0(x)$ is linear function of macro-variable in formula

(11), that is to say, second and higher order partial differential derivatives of $\mathbf{u}^0(x)$ are all zeros. And then the displacement vector is written as

$$\mathbf{u}^\varepsilon(x, \omega) = \mathbf{u}^0(x) + \varepsilon \mathbf{N}_{\alpha_1}(\xi, \omega) \frac{\partial \mathbf{u}^0(x)}{\partial x_{\alpha_1}} \quad (12)$$

where $\xi = \frac{x}{\varepsilon}$.

And then, the formulas on the strains inside previous column are exactly expressed as

$$\varepsilon_{hk}(x, \omega) = \frac{1}{2} \left(\frac{\partial u_h^0(x)}{\partial x_k} + \frac{\partial u_k^0(x)}{\partial x_h} \right) + \frac{1}{2} \left[\frac{\partial N_{\alpha_1 hm}(\xi, \omega)}{\partial \xi_k} + \frac{\partial N_{\alpha_1 km}(\xi, \omega)}{\partial \xi_h} \right] \frac{\partial u_m^0(x)}{\partial x_{\alpha_1}} \quad (13)$$

Substituting (11) into (13) and respecting the symmetry of $\mathbf{N}_{\alpha_1}(\xi, \omega^s)$, the expressions on the strain tensor are obtained inside any cell of the column

$$\begin{aligned} \varepsilon_{11}(x, \omega) &= -\frac{\nu_{13}}{E_{11}} p + p \frac{\partial}{\partial \xi_1} \left(\frac{1}{E_{33}} N_{313} - \frac{\nu_{13}}{E_{11}} N_{111} - \frac{\nu_{23}}{E_{22}} N_{212} \right) (\xi, \omega) \\ \varepsilon_{12}(x, \omega) &= \frac{p}{2} \frac{\partial}{\partial \xi_1} \left(\frac{1}{E_{33}} N_{323} - \frac{\nu_{13}}{E_{11}} N_{121} - \frac{\nu_{23}}{E_{22}} N_{222} \right) (\xi, \omega) \\ &\quad + \frac{p}{2} \frac{\partial}{\partial \xi_2} \left(\frac{1}{E_{33}} N_{313} - \frac{\nu_{13}}{E_{11}} N_{111} - \frac{\nu_{23}}{E_{22}} N_{212} \right) (\xi, \omega) \\ \varepsilon_{13}(x, \omega) &= \frac{p}{2} \frac{\partial}{\partial \xi_1} \left(\frac{1}{E_{33}} N_{333} - \frac{\nu_{13}}{E_{11}} N_{131} - \frac{\nu_{23}}{E_{22}} N_{232} \right) (\xi, \omega) \\ &\quad + \frac{p}{2} \frac{\partial}{\partial \xi_3} \left(\frac{1}{E_{33}} N_{313} - \frac{\nu_{13}}{E_{11}} N_{111} - \frac{\nu_{23}}{E_{22}} N_{212} \right) (\xi, \omega) \\ \varepsilon_{22}(x, \omega) &= -\frac{\nu_{23}}{E_{22}} p + p \frac{\partial}{\partial \xi_2} \left(\frac{1}{E_{33}} N_{323} - \frac{\nu_{13}}{E_{11}} N_{121} - \frac{\nu_{23}}{E_{22}} N_{222} \right) (\xi, \omega) \\ \varepsilon_{23}(x, \omega) &= \frac{p}{2} \frac{\partial}{\partial \xi_2} \left(\frac{1}{E_{33}} N_{333} - \frac{\nu_{13}}{E_{11}} N_{131} - \frac{\nu_{23}}{E_{22}} N_{232} \right) (\xi, \omega) \\ &\quad + \frac{p}{2} \frac{\partial}{\partial \xi_3} \left(\frac{1}{E_{33}} N_{323} - \frac{\nu_{13}}{E_{11}} N_{121} - \frac{\nu_{23}}{E_{22}} N_{222} \right) (\xi, \omega) \\ \varepsilon_{33}(x, \omega) &= \frac{p}{E_{33}} + p \frac{\partial}{\partial \xi_3} \left(\frac{1}{E_{33}} N_{333} - \frac{\nu_{13}}{E_{11}} N_{131} - \frac{\nu_{23}}{E_{22}} N_{232} \right) (\xi, \omega) \end{aligned} \quad (14)$$

where $\xi = \frac{x}{\varepsilon}$.

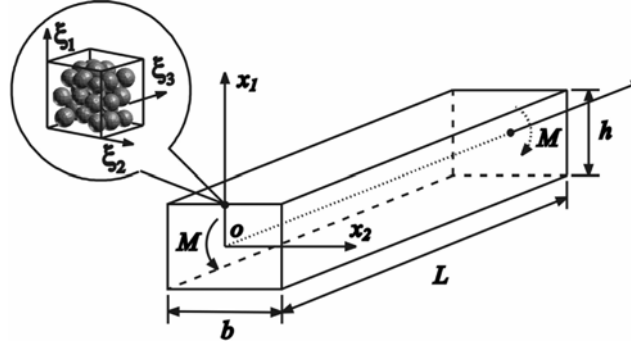


Fig 4. The bending of cantilever

Furthermore, from above strains expressions (14) the stresses are evaluated anywhere inside every cell in the column. Then based on the yield criterion of basic materials, such as the matrix, the core and shell of particle, the critical point of tensile column of CPPC is evaluated.

b) Beam bending

The bending of the cantilever with rectangular cross section is studied, as shown in Fig. 4. $x_3 = 0$ denotes fixed end and at $x_3 = L$ the bending moment round x_2 axis is imposed. From solid mechanics, the bending problem of the cantilever with orthogonal-anisotropic material coefficients has following solutions

$$\begin{cases} u_1^0 = -\frac{M}{2I_{x_2}} \left(\frac{1}{E_{33}} x_3^2 + \frac{\nu_{13}}{E_{11}} x_1^2 - \frac{\nu_{23}}{E_{22}} x_2^2 \right) \\ u_2^0 = -\frac{\nu_{23}M}{E_{22}I_{x_2}} x_1 x_2 \\ u_3^0 = \frac{M}{E_{33}I_{x_2}} x_1 x_3 \end{cases} \quad (15)$$

where $I_{x_2} = \frac{bh^3}{12}$ is the moment of inertia round x_2 .

Obviously, the above displacement $\mathbf{u}^0(x)$ is quadratic function of macro-variable, that is to say, third and higher order derivatives of $\mathbf{u}^0(x)$ are all zeros. So the displacement vector of the bending problem of the cantilever made from CPPC is written as

$$\mathbf{u}^\varepsilon(x, \omega) = \mathbf{u}^0(x) + \varepsilon \mathbf{N}_{\alpha_1}(\xi, \omega) \frac{\partial \mathbf{u}^0(x)}{\partial x_{\alpha_1}} + \varepsilon^2 \mathbf{N}_{\alpha_1 \alpha_2}(\xi, \omega) \frac{\partial^2 \mathbf{u}^0(x)}{\partial x_{\alpha_1} \partial x_{\alpha_2}} \quad (16)$$

Thus the strains anywhere inside above cantilever are calculated by the following formulas

$$\begin{aligned}
\varepsilon_{hk}(x, \omega) &= \frac{1}{2} \left(\frac{\partial u_h^0(x)}{\partial x_k} + \frac{\partial u_k^0(x)}{\partial x_h} \right) \\
&+ \varepsilon \frac{1}{2} \left[N_{\alpha_1 hm}(\xi, \omega) \frac{\partial^2 u_m^0(x)}{\partial x_{\alpha_1} \partial x_k} + N_{\alpha_1 km}(\xi, \omega) \frac{\partial^2 u_m^0(x)}{\partial x_{\alpha_1} \partial x_h} \right] \\
&+ \frac{1}{2} \left[\frac{\partial N_{\alpha_1 hm}(\xi, \omega)}{\partial \xi_k} + \frac{\partial N_{\alpha_1 km}(\xi, \omega)}{\partial \xi_h} \right] \frac{\partial u_m^0(x)}{\partial x_{\alpha_1}} \\
&+ \varepsilon \frac{1}{2} \left[\frac{\partial N_{\alpha_1 \alpha_2 hm}(\xi, \omega)}{\partial \xi_k} + \frac{\partial N_{\alpha_1 \alpha_2 km}(\xi, \omega)}{\partial \xi_h} \right] \frac{\partial^2 u_m^0(x)}{\partial x_{\alpha_1} \partial x_{\alpha_2}}
\end{aligned} \tag{17}$$

Further, respecting the symmetry of $\mathbf{N}_{\alpha_1}(\xi, \omega)$ and $\mathbf{N}_{\alpha_1 \alpha_2}(\xi, \omega)$, the components of strain tensor inside the cantilever are expressed as follows

$$\begin{aligned}
\varepsilon_{11}(x, \omega) &= \varepsilon \frac{M}{I_{x_2}} \left(\frac{1}{E_{33}} N_{313}(\xi, \omega) - \frac{\nu_{23}}{E_{22}} N_{212}(\xi, \omega) - \frac{\nu_{13}}{E_{11}} N_{111}(\xi, \omega) \right) \\
&+ \frac{Mx_1}{I_{x_2}} \frac{\partial}{\partial \xi_1} \left(\frac{1}{E_{33}} N_{313} - \frac{\nu_{23}}{E_{22}} N_{212} - \frac{\nu_{13}}{E_{11}} N_{111} \right) (\xi, \omega) \\
&+ \frac{\varepsilon M}{I_{x_2}} \frac{\partial}{\partial \xi_1} \left(\frac{1}{E_{33}} N_{3113} - \frac{\nu_{23}}{E_{22}} N_{2112} - \frac{\nu_{13}}{E_{11}} N_{1111} \right) (\xi, \omega) - \frac{\nu_{13} Mx_1}{E_{11} I_{x_2}} \\
\varepsilon_{12}(x, \omega) &= \varepsilon \frac{M}{2I_{x_2}} \left(\frac{1}{E_{33}} N_{323}(\xi, \omega) - \frac{\nu_{23}}{E_{22}} N_{222}(\xi, \omega) - \frac{\nu_{13}}{E_{11}} N_{121}(\xi, \omega) \right) \\
&+ \frac{Mx_1}{2I_{x_2}} \frac{\partial}{\partial \xi_1} \left(\frac{1}{E_{33}} N_{323} - \frac{\nu_{23}}{E_{22}} N_{222} - \frac{\nu_{13}}{E_{11}} N_{121} \right) (\xi, \omega) \\
&+ \frac{\varepsilon M}{2I_{x_2}} \frac{\partial}{\partial \xi_1} \left(\frac{1}{E_{33}} N_{3123} - \frac{\nu_{23}}{E_{22}} N_{2122} - \frac{\nu_{13}}{E_{11}} N_{1121} \right) (\xi, \omega) \\
&+ \frac{Mx_1}{2I_{x_2}} \frac{\partial}{\partial \xi_2} \left(\frac{1}{E_{33}} N_{313} - \frac{\nu_{23}}{E_{22}} N_{212} - \frac{\nu_{13}}{E_{11}} N_{111} \right) (\xi, \omega) \\
&+ \frac{\varepsilon M}{2I_{x_2}} \frac{\partial}{\partial \xi_2} \left(\frac{1}{E_{33}} N_{3113} - \frac{\nu_{23}}{E_{22}} N_{2112} - \frac{\nu_{13}}{E_{11}} N_{1111} \right) (\xi, \omega) \\
\varepsilon_{13}(x, \omega) &= \varepsilon \frac{M}{2I_{x_2}} \left(\frac{1}{E_{33}} N_{333}(\xi, \omega) - \frac{\nu_{23}}{E_{22}} N_{232}(\xi, \omega) - \frac{\nu_{13}}{E_{11}} N_{131}(\xi, \omega) \right) \\
&+ \frac{Mx_1}{2I_{x_2}} \frac{\partial}{\partial \xi_1} \left(\frac{1}{E_{33}} N_{333} - \frac{\nu_{23}}{E_{22}} N_{232} - \frac{\nu_{13}}{E_{11}} N_{131} \right) (\xi, \omega)
\end{aligned}$$

$$\begin{aligned}
& + \frac{\varepsilon M}{2I_{x_2}} \frac{\partial}{\partial \xi_1} \left(\frac{1}{E_{33}} N_{3133} - \frac{\nu_{23}}{E_{22}} N_{2132} - \frac{\nu_{13}}{E_{11}} N_{1131} \right) (\xi, \omega) \\
& + \frac{Mx_1}{2I_{x_2}} \frac{\partial}{\partial \xi_3} \left(\frac{1}{E_{33}} N_{313} - \frac{\nu_{23}}{E_{22}} N_{212} - \frac{\nu_{13}}{E_{11}} N_{111} \right) (\xi, \omega) \\
& + \frac{\varepsilon M}{2I_{x_2}} \frac{\partial}{\partial \xi_3} \left(\frac{1}{E_{33}} N_{3113} - \frac{\nu_{23}}{E_{22}} N_{2112} - \frac{\nu_{13}}{E_{11}} N_{1111} \right) (\xi, \omega) \\
\varepsilon_{22}(x, \omega) = & \frac{Mx_1}{I_{x_2}} \frac{\partial}{\partial \xi_2} \left(\frac{1}{E_{33}} N_{323} - \frac{\nu_{23}}{E_{22}} N_{222} - \frac{\nu_{13}}{E_{11}} N_{121} \right) (\xi, \omega) \\
& + \frac{\varepsilon M}{I_{x_2}} \frac{\partial}{\partial \xi_2} \left(\frac{1}{E_{33}} N_{3123} - \frac{\nu_{23}}{E_{22}} N_{2122} - \frac{\nu_{13}}{E_{11}} N_{1121} \right) (\xi, \omega) - \frac{\nu_{23} Mx_1}{E_{22} I_{x_2}} \\
\varepsilon_{23}(x, \omega) = & \frac{Mx_1}{2I_{x_2}} \frac{\partial}{\partial \xi_2} \left(\frac{1}{E_{33}} N_{333} - \frac{\nu_{23}}{E_{22}} N_{232} - \frac{\nu_{13}}{E_{11}} N_{131} \right) (\xi, \omega) \\
& + \frac{\varepsilon M}{2I_{x_2}} \frac{\partial}{\partial \xi_2} \left(\frac{1}{E_{33}} N_{3133} - \frac{\nu_{23}}{E_{22}} N_{2132} - \frac{\nu_{13}}{E_{11}} N_{1131} \right) (\xi, \omega) \\
& + \frac{Mx_1}{2I_{x_2}} \frac{\partial}{\partial \xi_3} \left(\frac{1}{E_{33}} N_{323} - \frac{\nu_{23}}{E_{22}} N_{222} - \frac{\nu_{13}}{E_{11}} N_{121} \right) (\xi, \omega) \\
& + \frac{\varepsilon M}{2I_{x_2}} \frac{\partial}{\partial \xi_3} \left(\frac{1}{E_{33}} N_{3123} - \frac{\nu_{23}}{E_{22}} N_{2122} - \frac{\nu_{13}}{E_{11}} N_{1121} \right) (\xi, \omega) \\
\varepsilon_{33}(x, \omega) = & \frac{Mx_1}{I_{x_2}} \frac{\partial}{\partial \xi_3} \left(\frac{1}{E_{33}} N_{333} - \frac{\nu_{23}}{E_{22}} N_{232} - \frac{\nu_{13}}{E_{11}} N_{131} \right) (\xi, \omega) \\
& + \frac{\varepsilon M}{I_{x_2}} \frac{\partial}{\partial \xi_3} \left(\frac{1}{E_{33}} N_{3133} - \frac{\nu_{23}}{E_{22}} N_{2132} - \frac{\nu_{13}}{E_{11}} N_{1131} \right) (\xi, \omega) + \frac{Mx_1}{E_{33} I_{x_2}}
\end{aligned} \tag{18}$$

where $\xi = \frac{x}{\varepsilon}$.

Using the stress-strain relation, one can evaluate the stresses anywhere inside the cantilever.

c) Twist of column

The twist of the column with circle cross section is shown in Fig. 5. r denotes the radius of cross section, L is the length of the column, $x_3 = 0$ fixed end, and at $x_3 = L$ the twist moment is imposed. If the column is made from orthogonal anisotropic materials, the displacement solution is expressed as

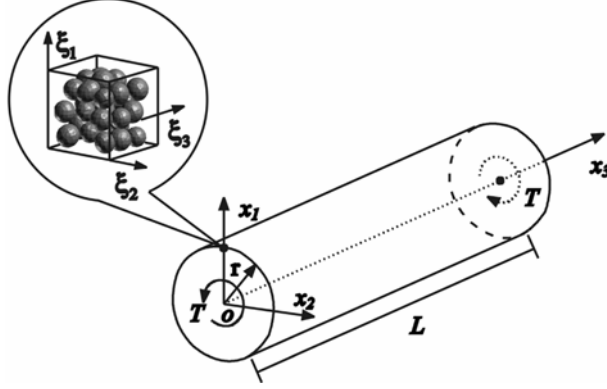


Fig. 5 Twist of the column with circle section

$$\begin{cases} u_1^0 = -\frac{Tx_2x_3}{\pi r^4} \left(\frac{1}{G_{13}} + \frac{1}{G_{23}} \right) \\ u_2^0 = \frac{Tx_1x_3}{\pi r^4} \left(\frac{1}{G_{13}} + \frac{1}{G_{23}} \right) \\ u_3^0 = -\frac{Tx_1x_2}{\pi r^4} \left(\frac{1}{G_{13}} + \frac{1}{G_{23}} \right) \end{cases} \quad (19)$$

where G_{13} , G_{23} denote the shear moduli in x_1 - x_3 plane and x_2 - x_3 plane. It is easy to see that the displacements are quadratic functions. And respecting the symmetry of $\mathbf{N}_{\alpha_1}(\xi, \omega)$ and $\mathbf{N}_{\alpha_1\alpha_2}(\xi, \omega)$ the components of strain tensor anywhere inside the twisting column are expressed as follows

$$\begin{aligned} \varepsilon_{11}(x, \omega) &= \frac{2\varepsilon T}{\pi r^4 G_{23}} N_{213}(\xi, \omega) + \frac{2T}{\pi r^4} \frac{\partial}{\partial \xi_1} \left(\frac{x_1}{G_{23}} N_{213} - \frac{x_2}{G_{13}} N_{113} \right) (\xi, \omega) \\ \varepsilon_{12}(x, \omega) &= \frac{\varepsilon T}{\pi r^4 G_{23}} (N_{223}(\xi, \omega) - N_{113}(\xi, \omega)) + \frac{T}{\pi r^4} \frac{\partial}{\partial \xi_1} \left(\frac{x_1}{G_{23}} N_{223} - \frac{x_2}{G_{13}} N_{123} \right) (\xi, \omega) \\ &\quad + \frac{T}{\pi r^4} \frac{\partial}{\partial \xi_2} \left(\frac{x_1}{G_{23}} N_{213} - \frac{x_2}{G_{13}} N_{113} \right) (\xi, \omega) \\ \varepsilon_{13}(x, \omega) &= \frac{\varepsilon T}{\pi r^4 G_{23}} N_{233}(\xi, \omega) - \frac{Tx_2}{\pi r^4 G_{13}} + \frac{T}{\pi r^4} \frac{\partial}{\partial \xi_1} \left(\frac{x_1}{G_{23}} N_{233} - \frac{x_2}{G_{13}} N_{133} \right) (\xi, \omega) \\ &\quad + \frac{T}{\pi r^4} \frac{\partial}{\partial \xi_3} \left(\frac{x_1}{G_{23}} N_{213} - \frac{x_2}{G_{13}} N_{113} \right) (\xi, \omega) \\ \varepsilon_{22}(x, \omega) &= -\frac{2\varepsilon T}{\pi r^4 G_{13}} N_{123}(\xi, \omega) + \frac{2T}{\pi r^4} \frac{\partial}{\partial \xi_2} \left(\frac{x_1}{G_{23}} N_{223} - \frac{x_2}{G_{23}} N_{123} \right) (\xi, \omega) \end{aligned}$$

$$\begin{aligned}
\varepsilon_{23}(x, \omega) &= \frac{Tx_1}{\pi r^4 G_{23}} - \frac{\varepsilon T}{\pi r^4 G_{13}} N_{133}(\xi, \omega) + \frac{T}{\pi r^4} \frac{\partial}{\partial \xi_2} \left(\frac{x_1}{G_{23}} N_{233} - \frac{x_2}{G_{13}} N_{133} \right) (\xi, \omega) \\
&\quad + \frac{T}{\pi r^4} \frac{\partial}{\partial \xi_3} \left(\frac{x_1}{G_{23}} N_{223} - \frac{x_2}{G_{13}} N_{123} \right) (\xi, \omega) \\
\varepsilon_{33}(x, \omega) &= \frac{2T}{\pi r^4} \frac{\partial}{\partial \xi_3} \left(\frac{x_1}{G_{23}} N_{233} - \frac{x_2}{G_{13}} N_{133} \right) (\xi, \omega)
\end{aligned} \tag{20}$$

where $\xi = \frac{x}{\varepsilon}$.

Using the stress-strain relation, one can evaluate the stresses anywhere inside the column. And then according to the yield criterion of the matrix, the core and shell of particle, the elasticity critical point of twist column of CPPC is evaluated.

3.2 Strength criterions

The elastic limit strength of CPPC is dominated by the elasticity strength of core, shell and matrix, specially, taking the Von-Mises effective stress yield criterion as the strength criterion for polymer matrix. For a fixed random sample ω^s , we apply STOTSM to the solution of strains and stresses in the investigated component, and then calculate the elastic limit strength value $S(\omega^s)$ of the sample ω^s by the proper strength criterions. The expected homogenized strength \hat{S} of the value $S(\omega^s)$ by Kolmogorov's strong law of large numbers is expressed as follows

$$\hat{S} = \frac{\sum_{s=1}^M S(\omega^s)}{M} \quad M \rightarrow +\infty \tag{21}$$

where M is the number of the samples.

The expected strength \hat{S} is only the average value of the component made from CPPC, so it doesn't manifest the strength performance enough. Actually in the component of random composites, the break of any cell may result in the elasticity performance failure of the structure. Therefore, the minimum value of all samples' strengths is more credible in practical engineering. It is expressed as follows

$$S_{min} = \min_{s=1, \dots, M} S(\omega^s) \tag{22}$$

4. Numerical modeling

In this section, the numerical modeling is discussed based on the description in section 2.1. Firstly, a new effective mesh generation algorithm is presented for the geometric model of meso-configuration in CPPC. Then an algorithm procedure of STOTSM is detailed.

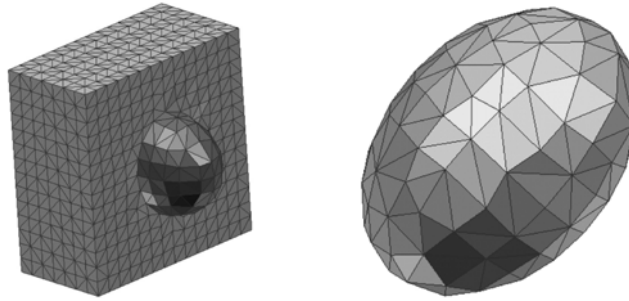


Fig. 6 The local effect of generated element meshes

4.1 Finite element meshes of tetrahedrons

The efficiency and quality to generate meshes have important influences on the efficiency and precision of STOTSM calculation. Therefore, a new mesh generation algorithm is developed for a geometric sample with random distribution model of ellipsoids. Firstly, the cube of a cell is divided into the uniform hexahedrons, namely Background Meshes. Secondly, we move the nodes of background meshes, which are very close to the ellipsoidal surface, onto the surface as more as possible, but it must be retained that the sides of background elements don't pass through the surface of ellipsoids. Thirdly, all of the background hexahedrons are divided into tetrahedrons under compatible condition. Finally, the coordinates of nodes of bad elements are locally adjusted to further improve the topology and qualities of the elements. Fig. 6 shows the local effect of generated meshes.

Hexahedral background meshes localizes the global mesh generation process, and it makes the tetrahedron generation only happens inside every hexahedron and relates to adjacent hexahedrons, and also the position shift of a node only affects the surrounding elements. Furthermore, sliver elements are treated and meshes are smoothed. As a result, it becomes possible to rapidly generate meshes of the cube with lots of random distribution ellipsoid.

4.2 Prismatic meshes for the shells of particles

The shell and core of a particle are regarded as an entire ellipsoid in section 2.1. Here, shells will be separated from the ellipsoids. In general the thicknesses of shells are all small. Due to this fact, all the nodes of tetrahedral elements in every ellipsoid are moved a little distance to approach the center of the ellipsoid by an affine transformation with equal proportion, but the nodes of matrix elements hold still. As a result that a space between the matrix and the shrunk ellipsoid emerges, and that is a shell of the particle. The shrinking operation leads to one to one correspondence between the nodes on internal and external surfaces of any shell. So, the triangular prism elements are generated by linking the corresponding nodes on internal and external surfaces (see Fig. 7(b)). Furthermore, refined mesh elements of the shells are obtained by dividing triangular prisms with equal proportion. Fig. 7 shows meshes of a cell with core-shell particles and the local shell elements.

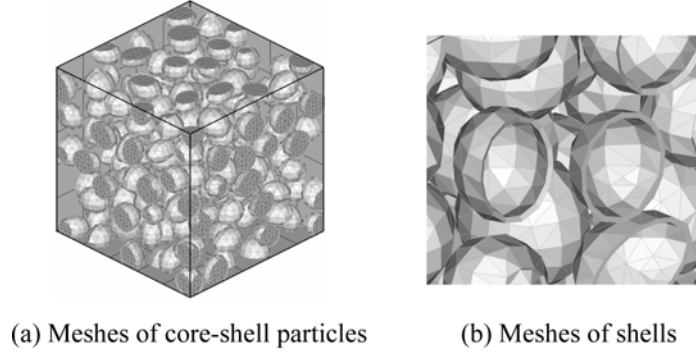


Fig. 7 Meshes in a cell

The high quality FE meshes are obtained by the above mesh generation algorithm (see Fig. 7(a)). The partition of the thin shell structure by triangular prisms is easier and more effective than by tetrahedrons, and also triangular prisms lead to fewer errors in finite elements computation than acute tetrahedron elements.

4.3 Algorithm procedure of STOTSM based on FEM

Based on the representation in section 2.1, the geometry modeling and FE mesh generation of CPPC in above section, the algorithm procedure for predicting the mechanics parameters of CPPC by STOTSM is following:

1. To generate a sample $\omega^s \in P$ of particle random distribution with given probability distribution model P in normalized cell Q^s , and then generate its FE meshes.
2. To solve the FE virtual work equation corresponding to Eq. (4) on 1-square Q to obtain $\mathbf{N}_{\alpha_1 m}(\xi, \omega^s)$, and then evaluate the homogenized constitutive coefficients $\{\hat{\alpha}_{ijk}(\omega^s)\}$ of sample ω^s by formula (5).
3. Repeat the steps from 1 to 2 for different samples $\omega^s \in P$ ($s = 1, 2, \dots, M$), M homogenized coefficients $\{\hat{\alpha}_{ijk}(\omega^s)\}$ are obtained. And then the expected homogenized coefficient $\{\bar{\alpha}_{ijk}\}$ is evaluated by Eq. (6).
4. If it's necessary, to evaluate $\mathbf{N}_{\alpha_1 \alpha_2 m}(\xi, \omega^s)$ ($\alpha_1, \alpha_2, m = 1, \dots, n$) by solving the FE virtual work equation corresponding to Eq. (7) on 1-square Q .
5. To obtain the homogenization displacement $\mathbf{u}^0(x)$ for typical component, or numerical displacement $\mathbf{u}^{0h}(x)$ for general structure by using FEM software, and then evaluate the high order partial derivatives $\frac{\partial^l u_m^{o,h}(x)}{\partial x_{\alpha_1} \cdots \partial x_{\alpha_l}}$.
6. For a determinate sample, using $\mathbf{N}_{\alpha_1 m}(\xi, \omega^s)$, $\mathbf{N}_{\alpha_1 \alpha_2 m}(\xi, \omega^s)$ and $\mathbf{u}^0(x)$ to calculate the stain and stress filed of structure Ω by Eqs. (9) and (10).
7. To evaluate the elastic limit strength $S(\omega^s)$ of sample ω^s according to the different strength criterions of matrix, core and shell.
8. For the all samples $\omega^s \in P$ ($s = 1, 2, \dots, M$), repeat the step 6 and 7 to obtain M strength parameters $S(\omega^s)$, and then to calculate the expected strength parameter and the minimum

strength parameter by Eqs. (26) and (27).

For the space limit, some skills on computing strains and stresses inside matrix, core and shell of each particle, are not described in detail by using FE methods in this paper.

5. Numerical experiments and results

In order to verify the availability and rationality of STOTSM for predicting CPPC, we have developed the software on the STOTSM, and made some numerical experiments for the mechanics parameters of CPPC in tension column, bending beam and twist column. Here some numerical results are shown and compared with experimental data.

Example 1:

This example is about the stiffness and strength parameter computation for tension case of CPPC column, and to compare with the experimental results in Wang *et al.* (2000). Table 1 summarizes the properties of the epoxy matrix and cores and shells of particles. And the overall density of a core-shell particle is 1.05 g/cm^3 in Wang *et al.* (2000). It supposes that the core-shell particle is MBS particle. Also, the core and shell are styrene butadiene rubber and poly (methyl methacrylate), respectively, and their densities are 0.95 g/cm^3 and 1.20 g/cm^3 . So, the ratio of shell's thickness value to radius of core-shell particle is 15% by mass conservation law. In paper Wang *et al.* (2000), it can be found that the overall modulus of a core-shell particle is 446 MPa, and the modulus of a rubber core is very small, only 2 MPa. Thus a core-shell particle can be regarded as a coreless particle, that is to say, the modulus of the shell approximate 446 MPa. Since the volume fraction of core-shell particles is relatively small in this paper, all lower than 25%, the break not happened in core and shell but in matrix is the main cause to the yielding behavior of investigated CPPC component under external force.

As a result, a relationship between the Young's modulus and the particle volume fraction is obtained by numerical prediction as illustrated in Fig. 8. STOTSM gives a stationary variation in the modulus with particle's volume fraction. Also, as the particle volume fraction increases, the modulus decreases. And then, the predicted values approximate the experimental results.

Fig. 9 shows the tensile strength values with different particle-filled volume fractions. Any predicted mean value in the figure is the average result of 50 random samples, so that the prediction is more credible. The figure illustrates the predicted strength value decreases as the volume fraction increases. On one hand, the predicted average strength values nearly approximate the experimental results; on the other hand, the predicted minimum values approach the lower limits of experimental data. Thus it can be seen that the predicted average values exactly reflect the variation of the real strength values, and also, the minimum values are more reliable in engineering practices.

Table 1 Material properties

	E (MPa)	ν
Matrix	3213	0.35
Core	2	0.49
Shell	446	0.37

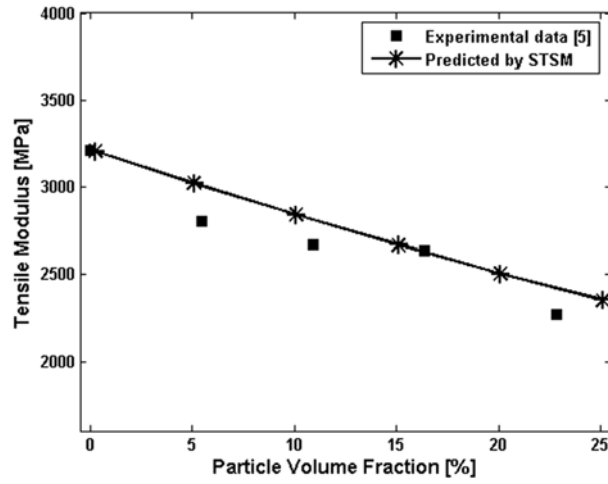


Fig. 8 Correlation of predicted tensile modulus with experimental results

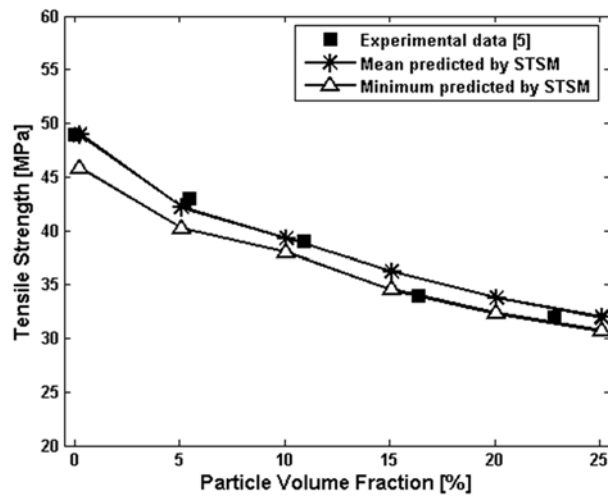


Fig. 9 Correlation of predicted tensile strength values with experimental results

Table 2 Material properties

	E (MPa)	ν
Epoxy	2600	0.35
PBA	2	0.49
PST	1400	0.40

Example 2:

As the comparison between the predicted values and experimental data in tension column in *example 1*, the predicted flexural moduli and strengths of CPPC are also satisfactory. In this example, the material parameters of PBA core, PST shell and epoxy matrix are shown in Table 2 Ormaetxea *et al.* (2001).

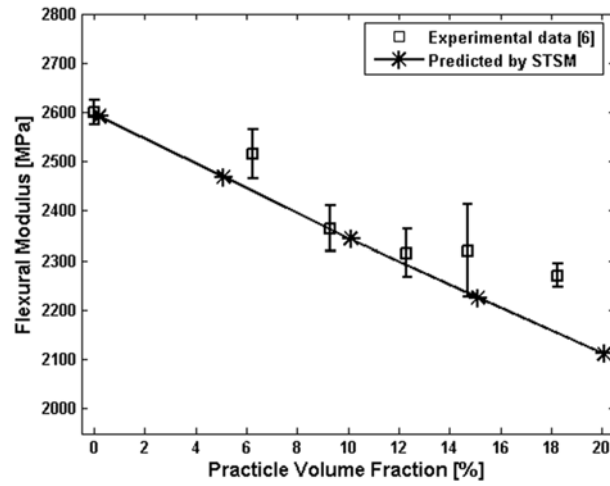


Fig. 10 Correlation of predicted flexural modulus with experimental results

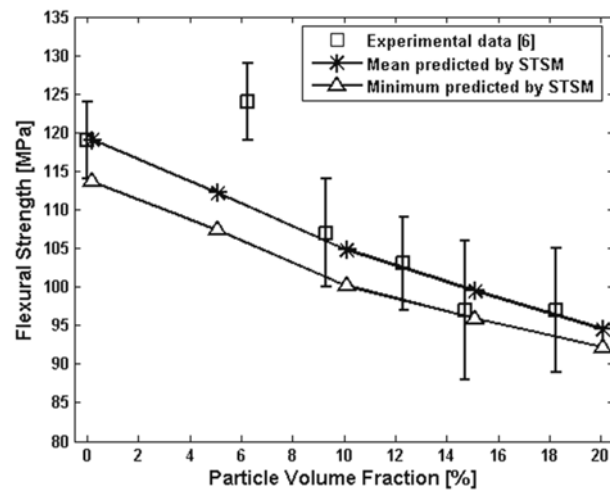


Fig. 11 Correlation of predicted flexural strength values with experimental results

As can be seen from Fig. 10, the predicted results accord with experimental data well. Fig. 11 depicts that the predicted flexural strength reduces steadily as the particle volume fraction increases. And the mean predicted curve passes through the centers of the experimental error bars, while the minimum curve decreases nearly along the lower limits of the error bars, where error bars come from the experimental data in paper (Ormaetxea *et al.* 2001). Therefore, it is further shown that the computed results reflect an average change of the real materials and the minimum values outline the lower limits of practical properties. They are more useful in engineering.

Example 3:

In this example, the tensile moduli and strengths with the different sizes of particles, the different compositions and weight ratios of core/shell, are compared. The composite materials are made from PST plastic, PBA rubber in core-shell particles and epoxy matrix Pérez-Carrillo *et al.* 2007. The main

computing parameters are following: the tensile strength of epoxy is 52 MPa, the density of PBA is 0.90 g/cm^3 , and that PST's is 0.96 g/cm^3 . The core-shell particles are uniformly distributed in the unit cell, and the particle's relative radiuses are 0.08 and 0.12. The volume fractions of particle are both 25%. The rest parameters are shown in Table 3, and then the calculated results of mechanical properties are revealed in Table 4.

The property of matrix keeps invariant in these examples, and the volume fraction of particles keeps 25%. As we know that the changes of the whole performance of a core-shell particle are reflected by property changes of the polymer composites. From table 4 the mechanics properties of core-shell particles are determined by the sizes of particles and the compositions of core and shell. The lateral comparison in the table shows that the particle becomes more rigid as the size reduces, that is, the modulus increases and both mean and minimum strength value rises. Paper Pérez-Carrillo *et al.* 2007 explains that the stress concentration increases with particle size, and the probability of finding a large flaw within a certain volume increases. As a result, the tensile strength decreases as the size rises. The material properties of the shell have more effects on the properties of particles than that of the core. When the material weight ratio in particles is the same, such as the ratio PST to PBA keeps 40/60 or 60/40, the overall property of particles, whose shell is plastic PST, is more rigid than that particle with PBA rubber shell. The weight ratio change leads to a more evident mechanics parameter change for particles made from hard shell (PST) and soft core (PBA) than soft shell and hard core. The stiffness and strength properties of particles with hard shell and soft core have less decrease than that with soft shell and hard core, as the size of the particles increase the same measure. The above prediction for mechanics properties by analyzing numerical results of STOTSM agree with that of experimental data in paper Pérez-Carrillo *et al.* 2007.

From the above examples, obviously, the STOTSM can be utilized to predict mechanics parameters of CPPC exactly, including the stiffness and the elastic limit strength. And the predicted values consist with the experimental data. Therefore, the STOTSM for the mechanics parameter prediction of CPPC is feasible.

Table 3 Material properties

	E (MPa)	ν
Epoxy	3200	0.35
PBA	2	0.49
PST	1400	0.40

Table 4 Numerical results of mechanical properties with different composition and particle size

Core/shell composition	Particle Radius 0.08 (in unit cube)				Particle Radius 0.12 (in unit cube)			
	Shell Thickness	E (MPa)	Mean Tensile Strength (MPa)	Minimum Tensile Strength (MPa)	Shell Thickness	E (MPa)	Mean Tensile Strength (MPa)	Minimum Tensile Strength (MPa)
PBA/PST 40/60	0.020	2528	38.28	36.78	0.030	2437	35.91	33.86
PBA/PST 60/40	0.012	2436	35.78	34.32	0.018	2335	33.17	31.11
PST/PBA 40/60	0.022	2324	32.98	31.43	0.033	2204	29.02	26.73
PST/PBA 60/40	0.013	2348	33.45	31.95	0.020	2233	29.62	27.62

6. Conclusions

In this paper, a Statistical Two-Order and Two-Scale Method (STOTSM) for mechanics parameters prediction of Core-shell Particle-filled Polymers Composites (CPPC) is developed based on two-order and two-scale asymptotic expression on the displacement solution of the structure made from composites with random particle distribution, and the related formulas are given. For the materials with random distribution of larger numbers of core-shell particles the stiffness parameters and elastic limit strength parameters have been predicted. The following conclusions are worked out:

- (1) The strength parameter of CPPC doesn't only depend on the macro-conditions, such as geometry of the structure, the loading and constraints, but also on micro-configuration, such as particle's size, composition and weight ratio of core/shell.
- (2) The consistencies of the predicted results with experimental data in tension and bending case of column show STOTSM is available to predict mechanics parameters of CPPC, including stiffness parameters, the expected strength and the minimum strength. The minimum strength value provides a more valuable reference for the available property of CPPC. Moreover, the influence of core-shell particle's configuration and composition on mechanics properties is obtained by analyzing the calculated results, which accords with experimental data. As a result, the information of micro-behaviors can be captured exactly by STOTSM prediction.
- (3) In this paper, a new effective mesh generation method is also presented for the geometric model. It can rapidly generate finite element meshes of investigated cell with a large number of random distributed core-shell particles. And it effectively supported the practical FE computation by STOTSM.

It should be mentioned that for the composite materials with random distribution of a great number of arbitrarily geometric particles the convergence of calculating the strength parameters has not been valid. In fact, if some particles are polyhedron, the strains and stresses near any corner point can not be more exactly calculated. The geometry modeling for micro/meso-configuration, mesh generation method and statistical two-order and two-scale method also can be applied to predict mechanics parameters of other core-shell particle-filled materials.

Acknowledgements

This work is supported by the Special Funds for Major State Basic Research Project (2005CB321704), the National Natural Science Foundation of China (10590353 and 90405016), and also supported by the center for high performance computing, NWPU in China.

References

- Yu, Y., Cui, J.Z. and Han, F. (2006), "An effective computer generation method for the materials with random distribution of large numbers of heterogeneous grains", *Computational Methods in Engineering and Science. Proceeding of the EPMESC X*, Sanya, China, pp. 273.
- Li, Y.Y. (2004), "Multi-Scale Algorithm Predicting Mechanical/Heat Transfer Parameters of the Composite Materials with Random Grain Distribution of Periodicity", *PhD Thesis*, Chinese academy of sciences, Beijing.

- Li, Y.Y. and Cui, J.Z. (2005), "The multi-scale computational method for mechanics parameters of composite materials with random grain distribution", *Composites Science and Technology*, **65**, 1447-1458.
- Cui, J.Z., Yu, X.G., Han, F. and Yu, Y. (2007), "Statistical Two-Scale Method for Strength Prediction of Composites with Random Distribution and Its Applications", 'Computational Mechanics' *Proceedings of ISCM 2007* Edited by Z.H.Yao and M.W. Yuan, July 30-August 1, 2007, Beijing, China, Tsinghua University and Springer, pp. 60-79.
- Wang, X.M., Xiao, K.Q. and Ye, L. et al. (2000), "Modelling of mechanical properties of core-shell rubber modified epoxies", *Acta Materialia*, **48**, 579-586.
- Ormaetxea, M., Forcada, J. and Mugika, F. et al. (2001), "Ultimate properties of rubber and core-shell modified epoxy matrices with different chain flexibilities", *J Mater. Sci.*, **36**, 845-852.
- Pérez-Carrillo, L.A., Puca, M. and Rabelero, M. et al. (2007), "Effect of particle size on the mechanical properties of polystyrene and poly (butyl acrylate) core/shell polymers", *Polymer*, **48**, 1212-1218.